Porter, R. (2015). Linearised water wave problems involving submerged horizontal plates. Applied Ocean Research, 50, 91-109. 10.1016/j.apor.2014.07.013

Available online at www.sciencedirect.com

ScienceDirect

Applied Ocean Research 00 (2014) 1–24

Journal Logo

# Linearised water wave problems involving submerged horizontal plates

R. Porter

*School of Mathematics, University of Bristol, Bristol, BS8 1TW, UK.*

**Abstract**

In this paper a number of related linearised water wave problems all involving thin submerged horizontal plates are considered. An integral transform approach is adopted and used to formulate integral equations in terms unknown functions related to the jump in pressure across the plate. A Galerkin method is applied to the solution of these integral equations leading to elegant expressions for quantities of interest and a rapidly convergent numerical scheme. The focus of the paper is to demonstrate the application of this method in a number of settings including both two-dimensional problems applied to infinitely-long plates of constant width and three-dimensional problems involving circular discs. In the process we present new results including, for example, for wave-free forced oscillations of plates.

*Keywords:* Thin submerged horizontal plates, wave diffraction, wave radiation, integral equations.

## 1. Introduction

In this paper a number of problems relating to the interactions of surface gravity waves with thin horizontal plates are considered under the assumptions of linearised wave theory. These include: (i) the scattering of oblique waves by a plate of constant width; (ii) radiation from forced motion of plates and (iii) the scattering of waves by a circular plate. The main purpose of the paper is to demonstrate a new approach to solving a general class of problem involving thin submerged horizontal plates which has some advantages over existing solution methods.

The interaction of surface waves with submerged thin horizontal plates has been the subject of numerous studies over the past decades partly due to its potential application as either a submerged breakwater or underwater lens and partly because of an intrinsic interest in methods for solving boundary-value problems involving thin structures. Alongside numerical and experimental investigations, many different analytical solution methods and approximations have been developed. Some of the studies relevant to the current work will be listed below; many others are cited within these references.

Some solution methods are specific to the water depth being finite. For example, the popular eigenfunction matching method divides the fluid domain into four rectangular subdomains: above and below the plate and to the left and right of the plate. Expanding the velocity potential in each subdomain in terms of separation solutions and then matching velocities and pressure across common vertical boundaries leads to infinite systems of linear algebraic equations which can solved numerically by truncation. See, for example, McIver [1] or Mahmood-ul-Hassan *et al* [2]. As is often the case with so-called eigenfunction matching method, this approach is numerically intensive, requiring large series truncation sizes for modest levels of accuracy. This can be attributed to the fact that the method does

*Email address:* richard.porter@bris.ac.uk (R. Porter)

not explicitly take account of an essential requirement of the problem relating to the behaviour of the fluid at special points within fluid domain, in this case at the edges of the thin plates.

A variant of the eigenfunction matching method (in that it is based on the same domain decomposition) is the modified residue calculus approach (for a general description see Linton & McIver [3]) which *does* account for the specific behaviour at the edges of the plate. This sophisticated method gives identical results to those found from the Wiener-Hopf technique when applied to the problem of a semi-infinite plate where solutions are explicit (e.g. Greene & Heins [4], Heins [5]); this equivalence is explicitly demonstrated in Williams & Meylan [6].

For plates of finite length, Fernyhough [7] and Linton [8] showed that the residue calculus method results in systems of equations that are exponentially convergent. Additionally, when truncated to leading order, they are equivalent to a wide-spacing result which connects the scattering effects from the two edges of the plate using propagating waves only, assuming each edge is characterised by the scattering from a semi-infinite plate.

Alternative approaches include using Greens functions either in finite or infinite depth (see, for example, Linton & McIver [3]) where certain types of integral equation can be formulated. The main difficulty lies in how the integral equations are solved, and this is expanded upon further below.

There are also a number of approximations that are used. The wide-spacing approximation referred to above (e.g. McIver [1]), Linton & McIver [3]) is accurate when the wavelength over the plate is much less than the length of the plate. The shallow water approximation of Siew & Hurley [9] based on matched asymptotics accurately captures the solution in the long wavelength limit.

The method of solution presented here involves the use of either Fourier or Hankel transforms to formulate integral equations for functions related to the unknown jump in pressure across the plate. It is natural to consider transform methods when considering problems which possess coordinate-aligned geometry as is present here. The solution is approximated accurately and efficiently by use of a variational approach (Galerkin's method) in which the unknown is expanded in an orthogonal basis which incorporates the anticipated square-root behaviour in the pressure jump at the edges of the plate. Quantities of interest in the problem are readily expressed in terms of inner products involving the solutions to the integral equations and, consequently, are second order accurate due to the variational approximation adopted.

Perhaps unsurprisingly, there are a number of similarities in the approach presented here and methods based upon Greens functions referred to above. The present approach sets itself apart from previous work primarily in the way various equations are organised. The integral equation that is derived in this paper resulting from a transform approach is equivalent to the integral equation resulting from the use of a Greens function once its integral transform representation had been used. The introduction of a transform variable, either from the outset or, later, in a Greens function representation, is crucial to the present development and the ordering of domain and transform integrals allow the integral equation to be handled 'normally'. If the order of domain and transform integrals are reversed, the integral equations become hypersingular and immediately requires special attention. Hypersingular integral equations emerge naturally in the application of Green's functions to thin plates and can be dealt with by developing the appropriate machinery (e.g. Parsons & Martin [10], Parsons & Martin [11], Farina & Martin [12]) or by using 'regularisation methods' which integrate away the hypersingularity by switching normal to tangential derivatives to leave weakly singular integral equations (e.g. Porter [13]). This latter approach has some common features with the work of Grue & Palm [14] and Song & Faltinsen [15], for example, who use distributions of point vortices around submerged plates to formulate non-singular integral equations which are solved numerically after expanding the unknown vortex strength in terms of Fourier series. Many of the Greens function approaches described above have the advantage that they have been applied more generally to geometries where transforms are not appropriate. However, the main point of the present work is to demonstrate that this machinery is not necessary for the class of problem considered here.

In addition to the issue of the organisation of integral equations, we also show how it is possible to extract the dominant logarithmic singularity embedded in the integral equation, thus rendering it an integro-differential equation. Again, connections can be made to approaches described in the previous paragraph. For instance, the removal of the logarithmic singularity (the main component of the Greens function) is an essential part of the hypersingular integral equation approach, whilst the harmonicity of the function $\ln(r)$ ($r$ being radial distance) allows a switching of derivatives, and this bears some similarity to operations within the work of Porter [13], Grue & Palm [14]. The Galerkin method, too, is reminiscent of Porter [13], Grue & Palm [14] and some of the results used in the development of the numerical system of equations have similarities with the work on hypersingular integral equations although the body of work described in Parsons & Martin [10], Parsons & Martin [11], Farina & Martin [12] opt for collocation instead

of Galerkin methods. Farina & Martin [12] acknowledge that Galerkin methods are likely to provide simplication when their general method was applied to simplified geometries and they may well have anticipated a formulation similar to the one derived here. In particular they quote the work of Krenk & Schmidt [16] whose transformed-based integral equation coupled to a Galerkin approximation applied to circular disks in elasticity is essentially the same illustrated here for submerged disks in the water wave problem.

A by-product of the current approach is the development of an explicit long wavelength approximation to wave scattering by submerged horizontal plates, formally valid in $\kappa a \ll \pi$ where $\kappa$ will come to represent the wavenumber of travelling waves over the plate. This new approximation complements existing approximations which include the long-plate (or wide-spacing) approximation, formally valid for $\kappa a \gg \pi$ and the shallow-water approximation. The performance of these existing approximations is described in McIver [1] and is not a focus of attention here.

In Section 2, the scattering of waves by a fixed plate is considered in finite depth. The case of infinite depth is also found explicitly by letting the depth tend to infinity. Results are shown for reflection and transmission coefficients, demonstrating the rapid convergence of the numerical approximation with increasing number of terms in the series. In Section 3 the modification to the formulation is presented in the case of radiation of waves by the forced motion of the plate. Here we demonstrate that plates in heave or roll motions about the plate centre can produce local wave-free oscillations, and that off-centre rolling plates can radiate waves in one direction only. In Section 4 an integral equation formulation is derived for the three-dimensional extension of the plate to a submerged horizontal circular disc. There are some differences, particularly in the numerical solution method although the final numerical systems of equations are remarkably similar to that required in the two-dimensional problem.

## 2. Scattering of oblique waves by a submerged plate of constant width

Cartesian coordinates are used with $z = 0$ in the mean free surface and the fluid extending into $z < 0$. A thin horizontal plate is submerged to a depth $d$ in water of depth $h$. The plate extends horizontally from $x = -a$ to $x = a$ and uniformly in the $y$ direction. Assuming time-harmonic incident waves of angular frequency $\omega$ making an angle $\theta$ with respect to the positive $x$ direction, the governing equation to be satisfied by the velocity potential $\phi(x, z)$ is

$$(\nabla^2 - \beta^2)\phi(x, z) = 0, \qquad z < 0 \tag{1}$$

where $\beta = k \sin\theta$ where $k$ is the positive root of the dispersion relation

$$\omega^2/g \equiv K = k \tanh kh. \tag{2}$$

The velocity field is reconstructed from the gradient of $\Re\{\phi(x, z)e^{i(\beta y - \omega t)}\}$. In addition to (1), on the free surface

$$\phi_z - K\phi = 0, \qquad z = 0 \tag{3}$$

and on the lower boundary of the fluid,

$$\phi_z = 0, \qquad z = -h. \tag{4}$$

The condition to be applied on the plate is

$$\phi_z(x, -d^{\pm}) = 0, \qquad |x| < a. \tag{5}$$

We also define

$$\phi(x, -d^-) - \phi(x, -d^+) = \begin{cases} 0, & |x| \geq a \\ P(x), & |x| < a \end{cases} \tag{6}$$

and potential theory requires that $P(x) \sim C^{\pm}(a^2 - x^2)^{1/2}$ as $|x| \to a$ for constants $C^{\pm}$. In the case of infinite depth (2) holds in the limit $h \to \infty$ giving $k = K$, and (4) is replaced by

$$|\nabla\phi| = 0, \qquad z \to -\infty. \tag{7}$$

Finally radiation conditions are required as $|x| \to \infty$. We write

$$\phi(x, z) \sim \begin{cases} \phi_{inc}(x, z) + R\phi_{inc}(-x, z), & x \to -\infty \\ T\phi_{inc}(x, z), & x \to \infty \end{cases} \tag{8}$$

so that $R$ and $T$ are the complex reflection and transmission coefficients and

$$\phi_{inc}(x,z) = \mathrm{e}^{\mathrm{i}\alpha x}\psi(z) \tag{9}$$

where $\alpha = k\cos\theta$ and

$$\psi(z) = \begin{cases} \cosh k(z+h), & \text{(finite depth)}, \\ \mathrm{e}^{Kz}, & \text{(infinite depth)}. \end{cases} \tag{10}$$

The Fourier transform of the scattered part of the potential is defined by

$$\overline{\phi}(l,z) = \int_{-\infty}^{\infty} (\phi(x,z) - \phi_{inc}(x,z))\mathrm{e}^{-\mathrm{i}lx}\,dx \tag{11}$$

having the inverse

$$\phi(x,z) = \phi_{inc}(x,z) + \frac{1}{2\pi}\int_{-\infty}^{\infty} \overline{\phi}(l,z)\mathrm{e}^{\mathrm{i}lx}\,dl. \tag{12}$$

where the contour of integration in the inverse transform will be defined in order to satisfy the radiation condition.

Applying (11) to (1) gives

$$\left(\frac{d^2}{dz^2} - \gamma^2\right)\overline{\phi} = 0 \tag{13}$$

where $\gamma^2 = l^2 + \beta^2$ with

$$\left(\frac{d}{dz} - K\right)\overline{\phi} = 0, \qquad z = 0 \tag{14}$$

and either

$$\frac{d\overline{\phi}}{dz} = 0, \quad z = -h, \quad \text{or} \quad \overline{\phi} \to 0, \quad z \to -\infty, \tag{15}$$

depending on whether the fluid is finite or infinite depth (respectively). It is assumed in what follows that the fluid is of finite depth and we comment later on the changes required for infinite depth. Finally, since $\phi_z$ is continuous across $z = -d$ for all $x$ including across the plate, $|x| < a$ – see (5) – it follows that

$$\overline{\phi}_z(l,-d^-) = \overline{\phi}_z(l,-d^+). \tag{16}$$

Taking Fourier transforms of (6) gives

$$\overline{\phi}(l,-d^-) - \overline{\phi}(l,-d^+) = \int_{-a}^{a} P(x)\mathrm{e}^{-\mathrm{i}lx}\,dx \equiv \overline{P}(l). \tag{17}$$

Solving (13) in $-d < z < 0$ with (14) and in $-h < z < -d$ with (15) before matching across $z = -d$ using (16), (17) gives

$$\overline{\phi}(l,z) = \begin{cases} \dfrac{\overline{P}(l)\sinh\gamma(h-d)(\gamma\cosh\gamma z + K\sinh\gamma z)}{(\gamma\sinh\gamma h - K\cosh\gamma h)}, & -d < z < 0, \\ \dfrac{\overline{P}(l)\cosh\gamma(z+h)(-\gamma\sinh\gamma d + K\cosh\gamma d)}{(\gamma\sinh\gamma h - K\cosh\gamma h)}, & -h < z < -d. \end{cases} \tag{18}$$

At this point is only remains to satisfy the final condition of (5) on the plate which only needs to be done from one side since continuity of $\phi_z$ across the plate has been incorporated into the tranformed solution (18). We take some time preparing the ground for this final part of the solution. First, taking inverse transforms of the representation (18) in $-d < z < 0$ using (12) gives

$$\phi(x,z) = \phi_{inc}(x,z) + \frac{1}{2\pi}\int_{-\infty}^{\infty} \frac{\overline{P}(l)\sinh\gamma(h-d)(\gamma\cosh\gamma z + K\sinh\gamma z)}{(\gamma\sinh\gamma h - K\cosh\gamma h)}\mathrm{e}^{\mathrm{i}lx}\,dl. \tag{19}$$

There are poles on the real $l$-axis at $l = \pm\alpha$ where $\gamma = k$ – see (2). The contour of integration is taken to pass over the pole at $l = -\alpha$ and under the pole at $l = \alpha$ in order to satisy the radiation condition that $\phi - \phi_{inc}$ is outgoing.

Specifically, as we let $x \to \pm\infty$ in (19) we can deform the contour into either the upper-half or lower-half $l$-plane, capturing the residues at the poles $l = \pm\alpha$ resulting in

$$\phi(x,z) \sim \phi_{inc}(x,z) + \frac{\mathrm{i}k\sinh k(h-d)}{2\alpha h N_0}\overline{P}(\alpha)\phi_{inc}(x,z), \qquad x \to \infty, \tag{20}$$

and

$$\phi(x,z) \sim \phi_{inc}(x,z) + \frac{\mathrm{i}k\sinh k(h-d)}{2\alpha h N_0}\overline{P}(-\alpha)\phi_{inc}(-x,z), \qquad x \to -\infty, \tag{21}$$

where $N_0 = \frac{1}{2}(1 + \sinh(2kh)/(2kh))$. Comparing (20), (21) with (8) we see that

$$T - 1 = \frac{\mathrm{i}k\sinh k(h-d)}{2\alpha h N_0}\overline{P}(\alpha), \quad \text{and} \qquad R = \frac{\mathrm{i}k\sinh k(h-d)}{2\alpha h N_0}\overline{P}(-\alpha). \tag{22}$$

This allows us to write (19) as a real Cauchy principal-value integral plus contributions from the two poles each being one half of the residues calculated in (20) and (21) and this leads to

$$\phi(x,z) = \tfrac{1}{2}(T+1)\phi_{inc}(x,z) + \tfrac{1}{2}R\phi_{inc}(-x,z) + \frac{1}{2\pi}\int_{-\infty}^{\infty} \frac{\overline{P}(l)\sinh\gamma(h-d)(\gamma\cosh\gamma z + K\sinh\gamma z)}{(\gamma\sinh\gamma h - K\cosh\gamma h)}\mathrm{e}^{\mathrm{i}lx}\,dl. \tag{23}$$

Next, we note that, for $-d < z < 0$,

$$\frac{\sinh\gamma(h-d)(\gamma\cosh\gamma z + K\sinh\gamma z)}{(\gamma\sinh\gamma h - K\cosh\gamma h)} \sim \tfrac{1}{2}\mathrm{e}^{-|l|(z+d)}, \qquad |l| \to \infty. \tag{24}$$

We also note the integral representation of the logarithm (Gradshteyn & Ryzhik [17, §3.943]) for $z + d > 0$

$$\log\sqrt{(x-x')^2 + (z+d)^2} = \tfrac{1}{2}\int_{-\infty}^{\infty} \frac{\mathrm{e}^{-|l|} - \mathrm{e}^{-|l|(z+d)}\mathrm{e}^{\mathrm{i}l(x-x')}}{|l|}dl. \tag{25}$$

Combining (24) and (25) with (23) after re-instating $P(x)$ from (17) gives

$$\begin{aligned}\phi(x,z) \quad = \quad & \tfrac{1}{2}(T+1)\phi_{inc}(x,z) + \tfrac{1}{2}R\phi_{inc}(-x,z) + \frac{1}{2\pi}\frac{\partial}{\partial z}\int_{-a}^{a} P(x')\log\sqrt{(x-x')^2+(z+d)^2}\,dx' \\ & + \frac{1}{2\pi}\int_{-\infty}^{\infty}\Big[\frac{\sinh\gamma(h-d)(\gamma\cosh\gamma z + K\sinh\gamma z)}{(\gamma\sinh\gamma h - K\cosh\gamma h)} - \tfrac{1}{2}\mathrm{e}^{-|l|(z+d)}\Big]\mathrm{e}^{\mathrm{i}lx}\int_{-a}^{a} P(x')\mathrm{e}^{-\mathrm{i}lx'}\,dx'\,dl \end{aligned} \tag{26}$$

for $-d < z < 0$. Despite looking complicated and cumbersome, we are now in a position to apply the condition (5), and this gives

$$(T+1)f_+(x) + Rf_-(x) = \frac{1}{\pi}\frac{d^2}{dx^2}\int_{-a}^{a} P(x')\log|x-x'|\,dx' + \frac{1}{2\pi}\int_{-\infty}^{\infty} E_\beta(l)\mathrm{e}^{\mathrm{i}lx}\int_{-a}^{a} P(x')\mathrm{e}^{-\mathrm{i}lx'}\,dx'\,dl \tag{27}$$

for $|x| < a$, where

$$f_\pm(x) \equiv \frac{\partial}{\partial z}\phi_{inc}(\pm x, -d) = k\sinh k(h-d)\mathrm{e}^{\pm\mathrm{i}\alpha x} \tag{28}$$

and

$$E_\beta(l) = \frac{2\gamma\sinh\gamma(h-d)(\gamma\sinh\gamma d - K\cosh\gamma d)}{(\gamma\sinh\gamma h - K\cosh\gamma h)} - |l|. \tag{29}$$

Note in (27) we have used

$$\left(\frac{\partial^2}{\partial x^2} + \frac{\partial^2}{\partial z^2}\right)\log\sqrt{(x-x')^2+(z+d)^2} = 0 \tag{30}$$

to switch from $z$ to $x$-derivatives (formally this must be done before the derivative condition is applied on $z = -d$.)

It helps to employ operator notation here, so we define the integro-differential operator $\mathcal{K}$ by

$$(\mathcal{K}P)(x) \equiv \frac{1}{\pi}\frac{d^2}{dx^2}\int_{-a}^{a} P(x')\log|x-x'|\,dx' + \frac{1}{2\pi}\int_{-\infty}^{\infty} E_\beta(l)\mathrm{e}^{\mathrm{i}lx}\int_{-a}^{a} P(x')\mathrm{e}^{-\mathrm{i}lx'}\,dx'\,dl \tag{31}$$

and then let $P_\pm(x)$ satisfy

$$(\mathcal{K}P_\pm)(x) = f_\pm(x), \qquad |x| < a \tag{32}$$

whence, it follows, from (27), that

$$P(x) = (T+1)P_+(x) + RP_-(x). \tag{33}$$

Also, from (28), (22) and the definition (17),

$$T - 1 = \frac{\mathrm{i}}{2\alpha h N_0}\langle P, f_+\rangle, \quad \text{and} \quad R = \frac{\mathrm{i}}{2\alpha h N_0}\langle P, f_-\rangle \tag{34}$$

where we have used angled brackets to denote the inner product

$$\langle u, v\rangle = \int_{-a}^{a} u(x)v^*(x)\,dx. \tag{35}$$

with the asterisk denoting complex conjugate. Using (33) in (34) results in

$$\left.\begin{aligned} R &= \mathrm{i}\mu(T+1)S_{+,-} + \mathrm{i}\mu R S_{-,-} \\ T &= 1 + \mathrm{i}\mu(T+1)S_{+,+} + \mathrm{i}\mu R S_{-,+} \end{aligned}\right\} \tag{36}$$

where we have defined $\mu = 1/(2\alpha h N_0)$ (real) and $S_{\pm,\pm} = \langle P_\pm, f_\pm\rangle$, the first $\pm$'s on the left-hand side corresponding the first on the right-hand side and so on. Solving (36) for $R$ and $T$ gives

$$\begin{pmatrix} T \\ R \end{pmatrix} = (\mathbf{I} - \mathrm{i}\mu\mathbf{S})^{-1}(\mathbf{I} + \mathrm{i}\mu\mathbf{S})\begin{pmatrix} 1 \\ 0 \end{pmatrix}, \qquad \mathbf{S} = \begin{pmatrix} S_{+,+} & S_{-,+} \\ S_{+,-} & S_{-,-} \end{pmatrix} \tag{37}$$

and $\mathbf{I}$ is the $2\times 2$ identity matrix. Properties of the operator $\mathcal{K}$ allow it to be shown that $S_{-,+} = S^*_{+,-}$, $S_{+,+} = S^*_{+,+}$ and $S_{-,-} = S^*_{-,-}$ (and hence $S_{+,+}$, $S_{-,-}$ are real). Thus $\mathbf{S}$ is Hermitian matrix. The structure of (37) implies the conservation of energy relation $|R|^2 + |T|^2 = 1$ is automatically satisfied; this is evident from premultiplication of (37) by the conjugate transpose vector $(T^*, R^*)$ using properties of $\mathbf{S}$.

### *2.1. Infinite depth*

The case of infinite depth can be treated in a similar manner and leads to exactly the same type of formulation but with

$$E_\beta(l) = \gamma - \gamma\left(\frac{\gamma+K}{\gamma-K}\right)\mathrm{e}^{-2\gamma d} - |l| \tag{38}$$

$$f_\pm(x) = K\mathrm{e}^{\pm\mathrm{i}\alpha x}\mathrm{e}^{-Kd} \tag{39}$$

and the previous definition of $\mu$ is replaced with $\mu = K/\alpha = \sec\theta$. The infinite depth formulation can also be arrived at by letting $h \to \infty$ in the finite-depth equations presented in §2, modulo a suitable rescaling of $P(x)$ and $f_\pm(x)$.

### *2.2. Numerical method*

For the purposes of determining $R$ and $T$, it remains to solve (37) for $P_\pm(x)$ and compute the matrix $\mathbf{S}$ of inner products. Such a formulation is well suited to the Galerkin method.

We write

$$P_\pm(x) = \sum_{n=0}^{\infty} \alpha_n^\pm p_n(x/a), \qquad |x| \le a \tag{40}$$

in terms of unknown coefficients $\alpha_n$ where

$$p_n(t) = \frac{\mathrm{e}^{\mathrm{i}n\pi/2}}{\pi(n+1)}(1-t^2)^{1/2}U_n(t), \tag{41}$$

and $U_n$ are second kind Chebychev polynomials satisfying the orthogonality relationship

$$\int_{-1}^{1}(1-t^2)^{1/2}U_n(t)U_m(t)\,dt = \tfrac{1}{2}\pi\delta_{mn} \tag{42}$$

(e.g. Gradshteyn & Ryzhik [17, §7.34]). For practical purposes, the infinite series in (40) is truncated leading to an approximation to $P_\pm(x)$. Other useful results that can be inferred from Gradshteyn & Ryzhik [17, §7.34/5] include

$$\frac{d^2}{dt^2}\int_{-1}^{1}\ln|t-t'|(1-t'^2)^{1/2}U_n(t')dt' = \pi(n+1)U_n(t), \qquad |t|\le 1 \tag{43}$$

and

$$\int_{-1}^{1}\mathrm{e}^{\mathrm{i}\sigma t}(1-t^2)^{1/2}U_n(t)\,dt = \frac{\mathrm{e}^{\mathrm{i}n\pi/2}(n+1)\pi}{\sigma}J_{n+1}(\sigma) \tag{44}$$

the former of which demonstrates that the orthogonal polynomials $U_n$ are a natural choice, being eigenfunctions of the most singular part of the integro-differential operator in (31).

The Galerkin procedure involves substituting (40) into (32), multiplying through by $p_m^*(x/a)$ and integrating over $-a < x < a$. This results in the infinite system of equations for the unknown coefficients $\alpha_n^\pm$:

$$\frac{\alpha_m^\pm}{2\pi(m+1)} + \sum_{n=0}^{\infty}\alpha_n^\pm K_{m,n} = F_m^\pm, \qquad m = 0,1,2,\ldots \tag{45}$$

where

$$K_{m,n} = \frac{1}{2\pi}\int_{-\infty}^{\infty}\frac{E_\beta(l)}{l^2}J_{n+1}(la)J_{m+1}(la)\,dl \tag{46}$$

and

$$F_m^\pm = k\sinh k(h-d)\int_{-a}^{a}\mathrm{e}^{\pm\mathrm{i}\alpha x}p_m^*(x/a)\,dx = (\pm1)^m k\sinh k(h-d)\frac{J_{m+1}(\alpha a)}{\alpha}. \tag{47}$$

Noting that $K_{mn} = 0$ if $m+n$ implies a decoupling of (45) into its symmetric and antisymmetric parts for $\alpha_{2n}^\pm$ and $\alpha_{2n+1}^\pm$, thus

$$\frac{\alpha_{2m+\nu}^\pm}{2\pi(2m+1+\nu)} + \sum_{n=0}^{\infty}\alpha_{2n+\nu}^\pm K_{2m+\nu,2n+\nu} = F_{2m+\nu}^\pm, \qquad m = 0,1,2,\ldots \tag{48}$$

for $\nu = 0, 1$ where

$$K_{2m+\nu,2n+\nu} = \frac{1}{\pi}\int_0^{\infty}\frac{E_\beta(l)}{l^2}J_{2n+1+\nu}(la)J_{2m+1+\nu}(la)\,dl. \tag{49}$$

Note that (48) are real symmetric systems of equations and, since $F_m^- = (-1)^m F_m^+$, it follows that $a_m^- = (-1)^m a_m^+$ and it is therefore sufficient to find just the solution of (48) for $a_m^+$.

We also have

$$S_{\pm,\pm} = \langle P_\pm, f_\pm\rangle = \sum_{n=0}^{\infty}\alpha_n^\pm F_n^\pm \tag{50}$$

using (40), (47) and so

$$S_{+,+} = S_{-,-} = \sum_{n=0}^{\infty}\alpha_{2n}^+F_{2n}^+ + \sum_{n=0}^{\infty}\alpha_{2n+1}^+F_{2n+1}^+ \tag{51}$$

whilst

$$S_{+,-} = S_{-,+} = \sum_{n=0}^{\infty}\alpha_{2n}^+F_{2n}^+ - \sum_{n=0}^{\infty}\alpha_{2n+1}^+F_{2n+1}^+ \tag{52}$$

are also real.

Before continuing this is a good point at which to make a remark about the integro-differential equation formulation and its subsequent approximation. Earlier, efforts were made to remove the logarithmic singularity embedded in the integral representation (22) before applying the final boundary condition. As a result the integro-differential operator $\mathcal{K}$ emerged in (30) having a singular component and a regular part. It was shown that the result (43) allowed the singular part to be treated in such a way that it gave rise to the leading order term in the second-kind system of equations in (45). However, had we not extracted the logarithmic singularity the subsequent integral equation would have still been well-defined and we would have proceeded but with $E_\beta(l)$ replaced by $E_\beta(l) + |l|$. Subsequently, a first-kind system of equations would have resulted, replacing (45). However, an integral result (see (110) later) would have allowed us to integrate the $|l|$ component of $E_\beta(l) + |l|$ explicitly and the result of this evaluation would have resulted in precisely (45). In short, it is possible (and actually much easier) to arrive at the same algebraic system of equations without the need to identify and extract the logarithm from the integral representation of the potential. This observation provides useful insight and helps later with circular plates where the identification of the singularity is not made, but a second kind system still results, via the same mechanism described above.

### *2.3. Transparency in 2D*

Transparency requires $R = 0$ and $T = 1$, implying that far from the plate the incident wave without a phase shift is observed. The easiest way of seeing how to implement these conditions is to return to (22) which implies $\overline{P}(\pm\alpha) = 0$ and then this requires numerically that

$$\sum_{n=0}^{\infty} \alpha_n^+ F_n^+ = 0 \quad \text{and} \quad \sum_{n=0}^{\infty} (-1)^n \alpha_n^+ F_n^+ = 0 \tag{53}$$

or, alternatively,

$$\sum_{n=0}^{\infty} \alpha_{2n}^+ F_{2n}^+ = 0 \quad \text{and} \quad \sum_{n=0}^{\infty} \alpha_{2n+1}^+ F_{2n+1}^+ = 0. \tag{54}$$

It is also confirmed that $T = 1$ and $R = 0$ from (37) since (54) in (51), (52) implies $\mathbf{S} = 0$. The simultaneous satisfaction of the two real conditions (54) are sought as functions of plate parameters $a/d$, $d/h$ and frequency $Kh$ in the work of McIver *et al.* [18].

### *2.4. Wave exciting forces and moments*

A submerged fixed rigid plate is subject to a heave force $X_h$ and a roll moment (about its centre, say) $X_r$ due to the incident waves. These are given by weighted integrals of the pressure difference across the plates, so that

$$X_h = -\mathrm{i}\omega\rho \int_{-a}^{a} P(x)\, dx, \qquad \text{and} \qquad X_r = -\mathrm{i}\omega\rho \int_{-a}^{a} P(x) x\, dx, \tag{55}$$

respectively as functions of frequency. Using $f_0(x)$ to represent either the function 1 or the function $x$ we have

$$X_{h/r} = -\mathrm{i}\omega\rho((T+1)S_{+,0} + RS_{-,0}) \tag{56}$$

where $S_{\pm,0} = \langle P_\pm, f_0 \rangle$. In the case of heave $f_0 = U_0(x/a)$ and it follows using (40)–(42) that $S_{\pm,0} = \frac{1}{2} a \alpha_0^+$. For roll, $f_0 = \frac{1}{2} a U_1(x/a)$ and then $S_{\pm,0} = \mp \frac{1}{8} \mathrm{i} a^2 \alpha_1^+$. Note that the quantities $S_{\pm,0}$ will also arise later in relation to wave radiation problems. Thus we have

$$X_h = -\mathrm{i}\omega\rho \tfrac{1}{2} a \alpha_0^+ (R + T + 1) \qquad \text{and} \qquad X_r = \omega\rho \tfrac{1}{8} a^2 \alpha_1^+ (R - T - 1). \tag{57}$$

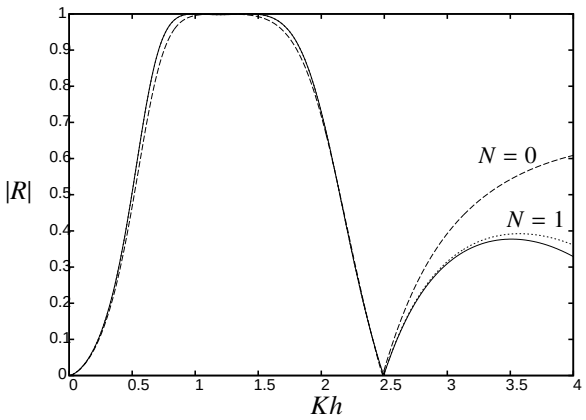


Figure 1. Modulus of the reflected wave amplitude as a function of $Kh = \omega^2 h/g$ for $d/h = 0.1$, $\beta = 0$ and $a/d = 5$. Solid curve $N = 10$; other values of $N$ shown against curves.

### 2.5. Results

First we describe the numerical method. The integrals defining $K_{mn}$ in (48) are computed by Guassian quadrature exploiting the rapid decay in the function $E_\beta(l)$ to truncate the infinite integral. When $\beta = 0$, the decay as $l \to \infty$ of $E_\beta$ is exponential with exponent $-l\min\{d, h-d\}$ whilst for oblique incidence the decay is algebraic and $O(1/|l|)$. The additional $l^3$ decay in the integrand implies that the decay for oblique incidence is $O(1/l^4)$. The numerical integration scheme is designed to compute $K_{mn}$ efficiently to eight significant figures.

The only other numerical parameter in the approximation is the truncation to $N$, say, of the series expansion in (40). We show in figures 1 and 2 the modulus of the reflection coefficient as a function of dimensionless frequency parameter, $Kh$, for two plates both with $d/h = 0.1, \beta = 0$ and with $a/d = 5$ and $a/d = 10$ respectively. These figures are chosen to replicate the results shown in McIver [1] figures 11 and 9 (respectively). The solid curves show the results computed using $N = 10$ and the remaining curves show the approximations as $N$ increases from zero, each curve being cut short at a frequency where accuracy has been lost.

We see that the $N = 0$, or single term, approximation (see §2.2) is accurate for low values of $Kh$ corresponding to long wavelengths. The wavelength of waves above the plate are given by $2\pi/\kappa$ where $\kappa$ is the wavenumber defined by the submergence $d$ via

$$K = \kappa \tanh \kappa d. \tag{58}$$

If $\kappa a \ll \pi$ (the wavelength over the plate is much greater than the length of the plate) we may expect the variation of $P_\pm(x)$ over $-a < x < a$ to be small and dominated by the square-root behaviour at the end points of the interval. As the number of wavelengths over the plate increases, the number of terms needed to accurately approximate $P(x)$ in (40) also increases.

In figures 3(a,b) we show the variation of the dimensionless wave exciting heave force $\hat{X}_h = |X_h|/(2\rho\omega a \cosh kh)$ and roll moment $\hat{X}_r = |X_r|/(4\rho\omega a^2 \cosh kh)$ with $\kappa a/\pi$ in the long wavelength regime with wave frequency set by $kh/2\pi = 0.016, \beta = 0$ and varying $\kappa a/\pi$. This choice is made to coincide with the parameters used in figures 14(a,c) in Patarapanich [19] who plotted long wavelength shallow water theory and compared with finite-element results. Our accruate computations based on an exact treatment of the problem compare favourably with those based on the shallow water approximation although there are expected noticeable quantitative differences, especially for larger plate lengths where zeros in the force and moment occur at slightly different frequencies. The agreement between shallow water and finite-element results suggested in Patarapanich [19] for $d/h = 0.3$ appear to be rather fortunate and agreement would not have been so great for $d/h = 0.1$ for example.

Although not commented upon in Patarapanich [19], or any subsequent work that the author is aware of, the zeros of heave force and roll moment imply, via the Haskind relations (see Mei [20]) zeros of wave radiation in the forced harmonic motion of a plate in heave and roll. This is explored further in §3.

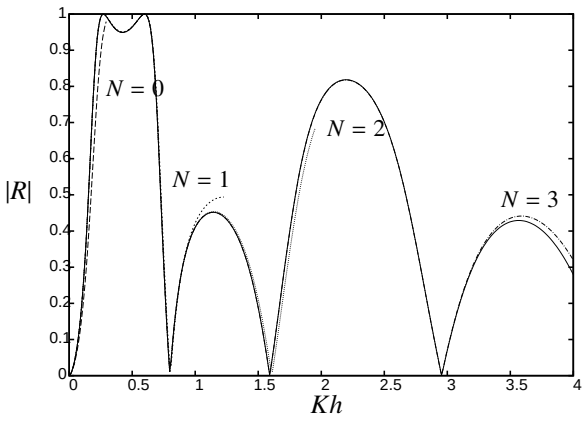


Figure 2. Modulus of the reflected wave amplitude as a function of $Kh = \omega^2 h/g$ for $d/h = 0.1$, $\beta = 0$ and $a/d = 10$. Solid curve $N = 10$; other values of $N$ shown against curves.

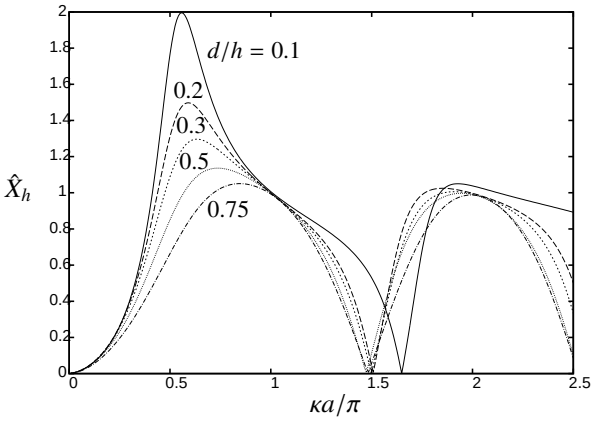


Figure 3. The dimensionless heave force $\hat{X}_h = |X_h|/(2\rho\omega a \cosh kh)$ as a function of $\kappa a/\pi$ for $kh/2\pi = 0.016$, $\beta = 0$ with $d/h$ varying from 0.1 to 0.75 (shown against curves).

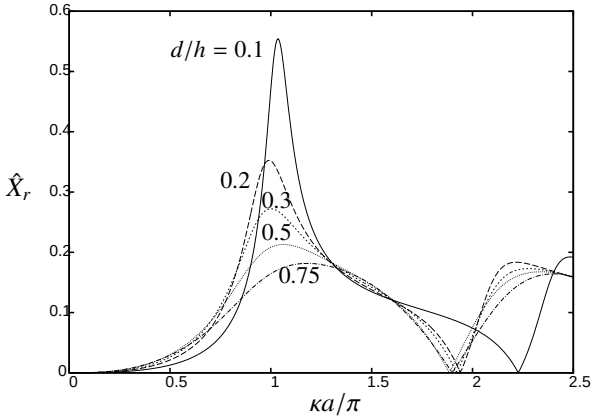


Figure 4. The dimensionless roll moment $\hat{X}_r = |X_r|/(4\rho\omega a^2 \cosh kh)$ about the centre of a plate as a function of $\kappa a/\pi$ for $kh/2\pi = 0.016$, $\beta = 0$ with $d/h$ varying from 0.1 to 0.75 (shown against curves).

## 3. Radiation of waves by forced motion

We envisage a two-dimensional problem ($\beta = 0$) in which the plate is forced to oscillate harmonically in time with angular frequency $\omega$ and spatially along the plate with a prescribed vertical velocity $-f_0(x)$, say, for $|x| < a$, where $f_0 \in \mathbb{C}$. For example, for a heaving plate $f_0(x) = 1$, and a plate rolling about $x = 0$, $f_0(x) = x$. For plates rolling about the point $x = c$, $f_0(x) = c - x$ and represents an in-phase combination of heave and roll.

There is no incident wave in this problem and the radiation condition (8) is replaced by

$$\phi(x,z) \sim \begin{cases} A_+\phi_{inc}(x,z), & x \to \infty, \\ A_-\phi_{inc}(-x,z), & x \to -\infty. \end{cases} \tag{59}$$

Otherwise, $\phi(x,z)$ satisfies (1) with $\beta = 0$ and (3), (4) with (5) replaced with

$$\phi_z(x,-d^{\pm}) = -f_0(x), \qquad |x| < a. \tag{60}$$

Fourier transforms are employed as before in the solution method but with the terms $\phi_{inc}$ relating to the incident wave removed from the definitions (11), (12) of the Fourier transforms as $\phi$ is already purely radiating in this example.

Following the procedure outlined for the scattering problem in §2, the contribution from the poles now means that (22) is replaced by

$$A_+ = \frac{\mathrm{i}k\sinh k(h-d)}{2\alpha hN_0}\overline{P}(\alpha), \quad \text{and} \qquad A_- = \frac{\mathrm{i}k\sinh k(h-d)}{2\alpha hN_0}\overline{P}(-\alpha) \tag{61}$$

and the integro-differential equation which results from applying (60) instead of (5) is

$$(\mathcal{K}P)(x) = 2f_0(x) + A_+f_+(x) + A_-f_-(x), \qquad |x| < a. \tag{62}$$

We decompose $P(x)$ writing

$$P(x) = 2P_0(x) + A_+P_+(x) + A_-P_-(x) \tag{63}$$

where $P_\pm(x)$ satisfy (32) in the scattering problem and where we also have $P_0(x)$ defined as the solution to

$$(\mathcal{K}P_0)(x) = f_0(x). \tag{64}$$

The result of using (63) in the two relations given by (61) and re-arranging for unknowns $A_\pm$ is

$$\begin{pmatrix} A_+ \\ A_- \end{pmatrix} = 2\mathrm{i}\mu\,(\mathbf{I} - \mathrm{i}\mu\mathbf{S})^{-1}\begin{pmatrix} S_{0,+} \\ S_{0,-} \end{pmatrix} \tag{65}$$

where $\mathbf{S}$ and $\mu = 1/(2khN_0)$ are defined by (37) as part of the scattering problem under normal incidence and

$$S_{0,\pm} = \langle P_0, f_\pm\rangle = \langle P_\pm, f_0\rangle^* \equiv S^*_{\pm,0}. \tag{66}$$

The second equality holds on account the self-adjointness of the operator $\mathcal{K}$. It follows that in order to calculate $A_\pm$ for a radiation problem, one only needs the solution $P_\pm$ of the scattering problem and use it to compute $S_{0,\pm}$ using the final equality in (66). According to the numerical procedure outlined in §2.3, (66) is represented by the summation

$$S^*_{\pm,0} = \sum_{n=0}^{\infty}\alpha_n^{\pm}F_n^0 = \sum_{n=0}^{\infty}\alpha_{2n}^{+}F_{2n}^0 \pm \sum_{n=0}^{\infty}\alpha_{2n+1}^{+}F_{2n+1}^0 \tag{67}$$

where

$$F_m^0 = \int_{-a}^{a} f_0(x)p_m^*(x)\,dx \tag{68}$$

is, in general, complex. Alternatively, if we expand $P_0(x)$ as

$$P_0(x) = \sum_{n=0}^{\infty}\alpha_n^0 p_n(x/a) \tag{69}$$

in (64) and employ the Galerkin approximation then the set of complex coefficients $\alpha^0_m$ are defined numerically by solving

$$\frac{\alpha^0_{2m+\nu}}{2\pi(2m+1+\nu)} + \sum_{n=0}^{\infty} \alpha^0_{2n+\nu} K_{2m+\nu,2n+\nu} = F^0_{2m+\nu}, \qquad m = 0, 1, 2, \ldots \tag{70}$$

for $\nu = 0, 1$ from which

$$S_{0,\pm} = \sum_{n=0}^{\infty} \alpha^0_n F^{\pm}_n = \sum_{n=0}^{\infty} \alpha^0_{2n} F^{+}_{2n} \pm \sum_{n=0}^{\infty} \alpha^0_{2n+1} F^{+}_{2n+1}. \tag{71}$$

For a heaving plate, $f_0(x) = 1 = U_0(x/a)$ then a simple calculation from (68) using (41), (42) shows that $F^0_m = \frac{1}{2}a\delta_{m0}$, whilst for roll, $f_0(x) = x = \frac{1}{2}aU_1(x/a)$ and then $F^0_m = -\frac{1}{8}\mathrm{i}a^2\delta_{m1}$. For combined roll and heave to give roll about $x = ca$, $f_0(x) = c - x$ gives $F^0_m = \frac{1}{2}ac\delta_{m0} + \frac{1}{8}\mathrm{i}a^2\delta_{m1}$. For a more general plate motion, one would expand $f_0(x)$ in the orthogonal basis $U_n(x/a)$.

### *3.1. Wave-free oscillations*

Of particular interest are forced motions which radiate waves in one direction only or, perhaps, do not radiate waves in either direction. The former is relevant to offshore wave energy where a simple time-reversal argument illustrates that a forced motion radiating waves in one direction only can also be used to absorb 100% of the energy in waves incident from that direction. Clearly, the forced oscillation must be unsymmetric about the centre of the plate otherwise the amplitudes of radiated waves in the two directions are necessarily equal. From (65) for there to be wave-free oscillations it is required that both $S_{0,\pm} = 0$, although if the forced motion is either symmetric or antisymmetric then $S_{0,+} = \pm S_{0,-}$ (respectively) and hence just one condition is required.

### *3.2. Added inertia and radiation damping coefficients*

The added inertia, $\mathcal{A}$, and radiation damping, $\mathcal{B}$, coefficients (per unit length) of the plate are defined as the real and imaginary parts of the integrated force/moment on the plate. In other words

$$\mathrm{i}\omega(\mathcal{A}+\mathrm{i}\mathcal{B}/\omega) = \mathrm{i}\omega\rho \int_{-a}^{a} P(x) f_0(x)\, dx = \mathrm{i}\omega\rho(A_+\langle P_+, f_0\rangle + A_-\langle P_+, f_0\rangle + 2\langle P_0, f_0\rangle) = \mathrm{i}\omega\rho(A_+ S_{+,0} + A_- S_{-,0} + 2S_{0,0}) \tag{72}$$

where

$$S_{0,0} = \langle P_0, f_0\rangle = \sum_{n=0}^{\infty} \alpha^0_n \left(F^0_n\right)^* \tag{73}$$

and this does require the solution of (70).

A simple reciprocity relation exists between the radiation damping coefficient and the far-field wave amplitudes of the form $\mathcal{B}/(\rho\omega) = \frac{1}{2}(|A_+|^2 + |A_-|^2)/\mu$ which can be used as a check on numerical method. Likewise the Haskind relation, which relates forces and moments due to incident waves on fixed structures to wave radiation in the direction of the incident wave. Here that relation is expressed in the form (see §2.4) $X_{h/r}/(\rho\omega) = -A^-/\mu$ where $f_0(x)$ is 1 for heave and $x$ for roll.

### *3.3. Results*

The reciprocal relations referred to in the paragraph above are satisfied exactly to within computational accuracy, independently of the number of terms, $N$, taken in the truncation of the infinite system.

For a small plate away from the surface and the bottom of the fluid the added inertia coefficients for low frequency oscillations should coincide with those for plates in an infinite fluid, which are $\rho\pi a^2$ in heave and $\frac{1}{8}\rho\pi a^4$ in roll. Numerical experiments not reported here have confirmed this.

In figure 5 we consider a heaving plate of length $a/d = 5$ in water depth $d/h = 10$. Three curves are shown against $\kappa a$ where $\kappa$ is the local wavenumber of propagating waves above the plate – see (58). The solid curve represents the wave radiated amplitudes $|A_\pm|/a$ whilst the dashed and dotted lines are the dimensionless added inertia and radiation damping coefficients. Note the usual relation between the two curves around 'resonance', the height of the radiation damping peak being approximately the same as the height of the jump in the added inertia, a typical feature explained

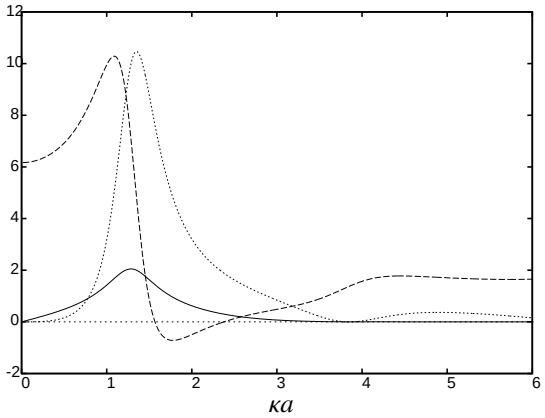


Figure 5. The dimensionless heave added inertia $\mathcal{A}/(\rho a^2)$ (dashed), damping $\mathcal{B}/(\rho\omega a^2)$ (dotted) and wave radiation amplitudes $|A_\pm|/a$ (solid) as a function of $\kappa a$, the dimensionless wavenumber over the plate with $a/d = 5$, $d/h = 0.1$.

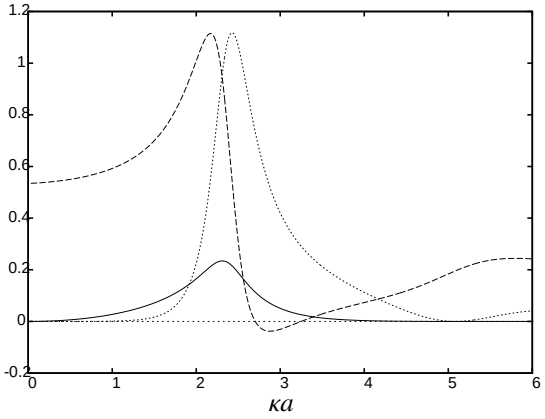


Figure 6. The dimensionless roll added inertia $\mathcal{A}/(\rho a^4)$ (dashed), damping $\mathcal{B}/(\rho\omega a^4)$ (dotted) and wave radiation amplitudes $|A_\pm|/a$ (solid) as a function of $\kappa a$, the dimensionless wavenumber over the plate with $a/d = 5$, $d/h = 0.1$.

by the Kramers-Kronig relations. Here resonance is associated approximately with $\kappa a = \pi/2$ so that there is approximately half a wavelength across the full extent of the plate, so that large motions lie at the centre of the plate and the antinodes of the oscillation lie at the edges of the plate. Note that the added inertia curve dips below zero, another common feature in hydrodynamics assoicated with bodies close to the free surface (McIver & Evans [**?** ]). There is also a value of $\kappa a \approx 3.850$ where $A_\pm = 0$, implying $\mathcal{B} = 0$, also. This is just one example of the general result that heaving plates possess frequencies of wave-free heaving oscillations.

In figure 6 we show the same set of results as in figure 5 with the same geometry but for the plate in roll motion instead of heave. Similar features emerge. So, for example, resonance is observed in for the rolling plate at approximately twice the wavenumber implying it is associated with wavelengths above the plate approximately equal to the plate. Now antinodes in this antisymmetric resonant oscillation lie at the centre of the plate and the two edges with large out-of-phase motions one quarter and three quarters of the way along the plate. Also note that, like the forced heave motion, the roll motion has zeros in the radiated wave amplitudes and damping, here at $\kappa a \approx 5.086$.

The wave-free oscillations in forced heave and roll motions numerically appear to exist for all plate sizes and depths of submergence although they become harder (graphically) to distinguish from near zero radiation when the plates become small or deeply submerged.

In the final example shown here, we consider in-phase combined roll and heave, equivalent to roll about a point about an arbitrary point $x = c$. When $c \neq 0$, the symmetry is broken and now $A_+ \neq A_-$, in general, and there is

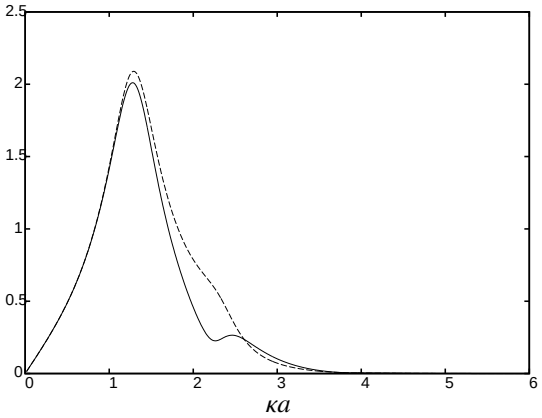


Figure 7. The dimensionless wave radiation amplitudes $|A_+|/a$ (solid) and $|A_-|/a$ (dashed) as a function of $\kappa a$, the dimensionless wavenumber over the plate with $a/d = 5$, $d/h = 0.1$ for a plate rolling about $x = c = a$.

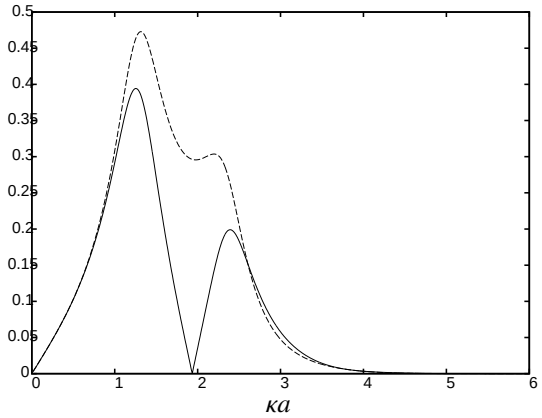


Figure 8. The dimensionless wave radiation amplitudes $|A_+|/a$ (solid) and $|A_-|/a$ (dashed) as a function of $\kappa a$, the dimensionless wavenumber over the plate with $a/d = 5$, $d/h = 0.1$ for a plate rolling about $x = c = 0.21a$.

wave radiation to both plus and minus infinity. For example, we have again considered $d/h = 0.1$ and $a/d = 5$ in figure 7 where the plate is rolling about the point $x = c = a$, the right-hand edge of the plate. One can see in the figure the competing effects of the two plate resonances associated with the heaving and rolling components. The figure confirms what is observed in other general configurations, that there are no frequencies of zero wave radiation to infinity.

However, in figure 8 we have selected, by numerical experimentation, a point along the length of the plate at $c \approx 0.210a$ where the rolling motion at a particular frequency $\kappa a \approx 1.934$ where $A_+ = 0$ and the waves are radiated in one direction only.

## 4. Scattering of waves by a thin submerged circular plate

We take Cartesian coordinates with $z = 0$ in the mean free surface and the fluid occupying $z < 0$. A thin circular plate of radius $a$ is submerged to a depth $d$ below the free surface in water of depth $h$ which may be infinite. Time-harmonic incident waves propagate in the direction of positive $x$. Polar coordinates $(r, \theta)$ are defined for this problem with $x = r\cos\theta$ and $y = r\sin\theta$. The velocity potential $\phi(r, \theta, z)$ describing the fluid motion satisfies

$$\nabla^2\phi = 0 \tag{74}$$

where, here, $\nabla^2$ represents the three-dimensional Laplacian, along with the same free surface and bottom conditions (3), (4) as in the two-dimensional problem. The condition on the plate is that

$$\frac{\partial}{\partial z}\phi(r,\theta,-d^{\pm}) = 0, \qquad r < a,\ 0 \le \theta < 2\pi. \tag{75}$$

We write the jump in the potential across $z = -d$ as

$$\phi(r,\theta,-d^{-}) - \phi(r,\theta,-d^{+}) = \begin{cases} 0, & r \ge a \\ P(r,\theta), & r < a \end{cases} \tag{76}$$

in terms of an unknown function $P(r,\theta)$ which has the behaviour $P(r,\theta) \sim C(\theta)(a^2 - r^2)^{1/2}$ as $r \to a^-$ in term of an unknown function $C(\theta)$. The incident wave is described by the potential

$$\phi_{inc} = \mathrm{e}^{\mathrm{i}kx}\psi(z) \equiv \psi(z)\sum_{n=0}^{\infty}\epsilon_n \mathrm{i}^n J_n(kr)\cos n\theta \tag{77}$$

where $\psi(z)$ is the depth variation given by (6), $\epsilon_n$ is 1 if $n = 1$ and 2 otherwise and $k$ satisfies (2).

The radiation condition requires that

$$\phi(r,\theta,z) - \phi_{inc}(r,\theta,z) \sim \sqrt{\frac{2}{\pi kr}}\mathrm{e}^{\mathrm{i}kr - \mathrm{i}\pi/4}A(\theta)\psi(z), \quad kr \to \infty \tag{78}$$

where $A(\theta)$ is the unknown complex diffraction coefficient.

On account of the circular symmetry and the fact that the incident wave can be decomposed into its angular Fourier modes we write

$$\phi(r,\theta,z) = \phi_{inc}(x,z) + \sum_{n=0}^{\infty}\epsilon_n \mathrm{i}^n \phi_n(r,z)\cos n\theta \tag{79}$$

and

$$A(\theta) = \sum_{n=0}^{\infty}\epsilon_n A_n \cos n\theta \tag{80}$$

(the factor $\mathrm{i}^n$ is suppressed for later algebraic convenience). Thus, $\phi_n(r,z)$ now satisfy, from (74)

$$\left(\frac{1}{r^2}\frac{\partial^2}{\partial r^2} + \frac{1}{r}\frac{\partial}{\partial r} - \frac{n^2}{r^2} + \frac{\partial^2}{\partial z^2}\right)\phi_n = 0 \tag{81}$$

along with the free surface and bottom conditions (3), (4) whilst (75) is replaced with

$$\frac{\partial \phi_n}{\partial z} = -J_n(kr)\psi'(-d) = -kJ_n(kr)\sinh k(h-d) \quad 0 < r < a \tag{82}$$

for the finite depth definition of $\psi(z)$. We also decompose $P(r,\theta)$ into Fourier modes, writing

$$P(r,\theta) = \sum_{n=0}^{\infty}\epsilon_n \mathrm{i}^n P_n(r)\cos n\theta \tag{83}$$

for $r < a$ so that

$$\phi_n(r,-d^{-}) - \phi_n(r,-d^{+}) = \begin{cases} 0, & r \ge a \\ P_n(r), & r < a \end{cases} \tag{84}$$

so that $P_n(r) \sim C_n(a^2 - r^2)^{1/2}$ as $r \to a$ for some constants $C_n$.

We introduce the Hankel Tranform

$$\overline{\phi}_n(\alpha,z) = \int_0^{\infty} r\phi_n(r,z)J_n(\alpha r)\,dr \tag{85}$$

with inverse

$$\phi_n(r,z) = \int_0^\infty \alpha \overline{\phi}_n(\alpha,z) J_n(\alpha r)\, d\alpha. \tag{86}$$

Taking Hankel transforms of (81) gives

$$\left(\frac{d^2}{dz^2} - \alpha^2\right)\overline{\phi}_n = 0 \tag{87}$$

whilst (3) and (4) gives

$$\left(\frac{d}{dz} - K\right)\overline{\phi}_n = 0, \qquad z = 0 \tag{88}$$

and

$$\frac{d\overline{\phi}_n}{dz} = 0, \qquad z = -h. \tag{89}$$

On account of $\phi_n(r,z)$ having a continuous $z$-derivative for all $r$, it follows that

$$\frac{d}{dz}\overline{\phi}_n(\alpha,-d^-) = \frac{d}{dz}\overline{\phi}_n(\alpha,-d^+) \tag{90}$$

whilst

$$\overline{\phi}_n(\alpha,-d^-) - \overline{\phi}_n(\alpha,-d^+) = \int_0^a rP_n(r)J_n(\alpha r)\, dr \equiv \overline{P}_n(\alpha). \tag{91}$$

The problem posed above for $\overline{\phi}_n(\alpha,z)$ is almost identical to that considered in §2 for the two-dimensional plate. Thus, the solution here is given by

$$\overline{\phi}_n(\alpha,z) = \begin{cases} \dfrac{\overline{P}_n(\alpha)\sinh\alpha(h-d)(\alpha\cosh\alpha z + K\sinh\alpha z)}{(\alpha\sinh\alpha h - K\cosh\alpha h)}, & -d < z < 0 \\ \dfrac{\overline{P}_n(\alpha)\cosh\alpha(z+h)(-\alpha\sinh\alpha d + K\cosh\alpha d)}{(\alpha\sinh\gamma h - K\cosh\alpha h)}, & -h < z < -d. \end{cases} \tag{92}$$

The solution is defined by its inverse transform and by imposing the final condition (82) from one side will determine the unknown $P_n(r)$. Thus we have, for $-d < z < 0$, the solution

$$\phi_n(r,z) = \int_0^\infty \alpha \frac{\overline{P}_n(\alpha)\sinh\alpha(h-d)(\alpha\cosh\alpha z + K\sinh\alpha z)}{(\alpha\sinh\alpha h - K\cosh\alpha h)} J_n(\alpha r)\, d\alpha. \tag{93}$$

The contour of integration is defined to go under the pole at $\alpha = k$ ensuring that waves are outgoing. Thus we find,

$$\phi_n(r,z) \sim \frac{\mathrm{i}\pi k\sinh k(h-d)\overline{P}_n(k)}{2hN_0} H_n^{(1)}(kr)\psi(z), \qquad kr \to \infty \tag{94}$$

where $H_n^{(1)}(kr)$ is the first kind Hankel function. Using the large argument asymptotics of this function,

$$H_n^{(1)}(kr) \sim \sqrt{\frac{2}{\pi kr}}\mathrm{e}^{\mathrm{i}(kr-\pi/4-n\pi/2)}, \qquad kr \to \infty$$

and comparing with the far-field form assumed for $\phi_n(r,z)$ shows that

$$A_n = \frac{\mathrm{i}\pi k\sinh k(h-d)\overline{P}_n(k)}{2hN_0}. \tag{95}$$

Now we write (93) as a real principal-value integral

$$\phi_n(r,z) = \fint_0^\infty \alpha \frac{\overline{P}_n(\alpha)\sinh\alpha(h-d)(\alpha\cosh\alpha z + K\sinh\alpha z)}{(\alpha\sinh\alpha h - K\cosh\alpha h)} J_n(\alpha r)\, d\alpha + A_n J_n(kr)\psi_n(z). \tag{96}$$

Unlike the development in §2 here it is not clear how to extract the most singular part of the representation above (in §2 we were able to identify a logarithm and, undoubtably, there is a singularity embedded in this representation also). In fact this does not matter, and need not have mattered in §2, as the removal of the singularity will happen 'algebraically' in the numerical systems of equations. Although this does not seem entirely rigorous or elegant it is an approach which simplifies the algebraic complexities associated with the removal of the singularity witness in the simpler two-dimensional formulation of §2.

Thus, we proceed instead by applying condition (85) to give the integral equation

$$2(1+A_n)f_n(r) = \int\!\!\!\!\!\!-_0^\infty \alpha(E_0(\alpha)+\alpha)J_n(\alpha r)\int_0^a P_n(s)J_n(\alpha s)s\,ds\,d\alpha \tag{97}$$

for $r < a$, after reinstating the definition of $\overline{P}_n(\alpha)$ from (91) where

$$f_n(r) = k\sinh k(h-d)J_n(kr) \tag{98}$$

and $E_0(\alpha)$ is defined in (29) of the two-dimensional problem with $\beta = 0$. We then define the scaled version of (97)

$$f_n(r) = \int\!\!\!\!\!\!-_0^\infty \alpha(E_0(\alpha)+\alpha)J_n(\alpha r)\int_0^a Q_n(s)J_n(\alpha s)s\,ds\,d\alpha \tag{99}$$

so that

$$P_n(r) = 2(1+A_n)Q_n(r). \tag{100}$$

Then it follows from (95)

$$A_n = \frac{\mathrm{i}\pi}{hN_0}(1+A_n)\langle Q_n, f_n\rangle \tag{101}$$

where, here, the angled brackets denote the inner product

$$\langle Q_n, f_n\rangle = k\sinh k(h-d)\int_0^a rQ_n(r)J_n(kr)\,dr. \tag{102}$$

The relation (101) can be rearranged to give $A_n$. Thus, we aim to approximate the solution $Q_n(s)$ to (99) and use it in (101), (102) to find $A_n$ and finally $A(\theta)$ from (80).

### *4.1. Numerical method*

We approximate the solution, $Q_n(s)$, to this integral equation using the Galerkin method. This involves substituting an expansion for the unknown function $Q_n(s)$ in a series of known functions. These should incorporate the known square-root behaviour at the edge of the disc, $r = a$. We write

$$Q_n(s) = \sum_{m=0}^{\infty}\alpha_m^{(n)}\Phi_m^{(n)}(s/a) \tag{103}$$

where

$$\Phi_m^{(n)}(x) = \frac{m!\Gamma(n+\frac12)}{\sqrt{2\pi}\Gamma(m+n+\frac32)}x^n C_{2m+1}^{n+1/2}(\sqrt{1-x^2}) \tag{104}$$

and $C_\mu^\nu(x)$ is the Gegenbauer polynomial. In particular, the functions $\Phi_m^{(n)}(x)$ incorporate the correct square-root behaviour at $x = 1$ and are orthogonal, satisfying

$$\int_0^1 \Phi_m^{(n)}(x)\Phi_l^{(n)}(x)\frac{x}{\sqrt{1-x^2}}\,dx = \begin{cases} 0, & m \neq l \\ \dfrac{(2m+2n+1)!(m!)^2}{4^n(2m+1)!(2m+n+\frac32)(\Gamma(m+n+\frac32))^2}, & m = l \end{cases} \tag{105}$$

which can be established from the definition (104) and the orthogonality relation for Gegenbauer polynomials. The numerical factors attached to $\Phi_m^{(n)}(x)$ are included to aid algebraic simplification – see (106) below.

Then, according to in Martin [22, equn. (4.9)] (who quotes Tranter [23] and Krenk [24]) we have the result

$$\int_0^1 \Phi_m^{(n)}(x) J_n(\xi x) x\, dx = \frac{J_{n+2m+3/2}(\xi)}{\xi^{3/2}}. \tag{106}$$

It follows that, after substituting the expansion for $Q_n(s)$ into the integral equation, and then multiplying through by $r\Phi_l^{(n)}(r/a)$ and integrating over $0 < r < a$, a process which characterises the application of the Galerkin method to the integral equation, results in the infinite system of equations

$$\sum_{m=0}^{\infty} \alpha_m^{(n)} K_{ml}^{(n)} = F_l^{(n)}, \qquad l = 0, 1, \ldots \tag{107}$$

where

$$K_{ml}^{(n)} = \int_0^{\infty} (E_0(\alpha) + \alpha) \frac{J_{n+2m+3/2}(\alpha a) J_{n+2l+3/2}(\alpha a)}{\alpha^2}\, d\alpha \tag{108}$$

and

$$F_l^{(n)} = \sinh k(h-d) \frac{J_{n+2l+3/2}(ka)}{(ka)^{1/2}}. \tag{109}$$

Both expressions above can be expressed alternatively in terms of spherical Bessel functions. Using a result from Gradshteyn & Ryzhik [17, §6.538(2)],

$$\int_0^{\infty} x^{-1} J_{\nu+2m+1}(x) J_{\nu+2l+1}(x)\, dx = \frac{\delta_{ml}}{(4l + 2\nu + 2)} \tag{110}$$

we may convert the first kind system of equations (107) into the second kind system

$$\frac{\alpha_l^{(n)}}{(4l+2n+3)} + \sum_{m=0}^{\infty} \alpha_m^{(n)} \widehat{K}_{ml}^{(n)} = F_l^{(n)}, \qquad l = 0, 1, \ldots \tag{111}$$

where

$$\widehat{K}_{ml}^{(n)} = \int_0^{\infty} \frac{E_0(\alpha)}{\alpha^2} J_{n+2m+3/2}(\alpha a) J_{n+2l+3/2}(\alpha a)\, d\alpha \tag{112}$$

involving an integrand with exponential decay.

The inner product in (102) is converted, upon substitution of (106), to

$$\langle Q_n, f_n \rangle = a \sum_{l=0}^{\infty} \alpha_l^{(n)} F_l^{(n)}. \tag{113}$$

The case of infinite depth can be considered most simply by explicitly taking the limits of $h \to \infty$, in a manner identical to that outlined in §2.

It is interesting to note there is very little difference between the systems (112) and (45). In particular we notice the relation

$$\widehat{K}_{ml}^{(n+2)} = \widehat{K}_{m+1,l+1}^{(n)} \tag{114}$$

which means the matrix elements only need to be computed for $n = 0$ and $n = 1$ and all subsequent $n$ are given, using (114) by $\widehat{K}_{ml}^{(2n)} = \widehat{K}_{m+n,l+n}^{(0)}$ and $\widehat{K}_{ml}^{(2n+1)} = \widehat{K}_{m+n,l+n}^{(1)}$. Identical relations are noted in a similar problem and treatment by Krenk & Schmidt [16].

If $\kappa a \ll \pi$ we argue, as before, that a one term truncation of the infinite system (107) should provide a good approximation to the solution and so

$$\alpha_0^{(n)} \approx F_0^{(n)} / ((2n+3)^{-1} + \widehat{K}_{00}^{(n)}) \tag{115}$$

and then (113) is approximated by

$$\langle Q_n, f_n \rangle \approx \frac{k^{-1} \sinh^2 k(h-d) \left(J_{n+3/2}(ka)\right)^2}{(2n+3)^{-1} + \displaystyle\int_0^{\infty} \frac{E_0(\alpha)}{\alpha^2} \left(J_{n+3/2}(\alpha a)\right)^2\, d\alpha}. \tag{116}$$

*4.2. Scattering cross section, forces and moments*

We define the scattering cross section as

$$\sigma = \frac{1}{2\pi}\int_0^{2\pi} |A(\theta)|^2\, d\theta = \sum_{n=0}^{\infty} \epsilon_n |A_n|^2 \tag{117}$$

following the use of (77). The so-called optical theorem (see Maruo [25]) states that

$$\sigma = -\Re\{A(0)\} = -\sum_{n=0}^{\infty} \epsilon_n \Re\{A_n\} \tag{118}$$

which provides an different way of calculating $\sigma$, although the definition (101) and the realness of $\langle Q_n, f_n\rangle$ implies (117) and (118) are equivalent.

The heave exciting force on the disk is given by

$$X_h = -\mathrm{i}\omega\rho \int_0^{2\pi}\int_0^a P(r) r dr\, d\theta = -2\pi\mathrm{i}\omega\rho \int_0^a P_0(r) r dr = -4\pi\mathrm{i}\omega\rho a^2(1+A_0)\sum_{m=0}^{\infty}\alpha_m^{(0)}\int_0^1 \Phi_m^{(0)}(t) t\, dt. \tag{119}$$

We note that from the definition (104) that $\Phi_0^{(0)} = \sqrt{2/\pi}(1-t^2)^{1/2}$ so

$$X_h = -\mathrm{i}\pi\sqrt{2\pi}\omega\rho a^2(1+A_0)\sum_{m=0}^{\infty}\alpha_m^{(0)}\int_0^1 \Phi_m^{(0)}(t)\Phi_0^{(0)}(t)\frac{t}{(1-t^2)^{1/2}}\, dt = -\mathrm{i}\omega\rho\tfrac{8}{3}\sqrt{2\pi}a^2(1+A_0)\alpha_0^{(0)} \tag{120}$$

after use of (105). A similar method applies to the roll moment, so that

$$X_r = -\mathrm{i}\omega\rho\int_0^{2\pi}\int_0^a P(r)(r\cos\theta) r dr\, d\theta = 2\pi\omega\rho\int_0^a P_1(r)\, r^2 dr = 4\pi\omega\rho a^3(1+A_1)\sum_{m=0}^{\infty}\alpha_m^{(1)}\int_0^1 \Phi_m^{(1)}(t)\, t^2\, dt \tag{121}$$

from the expansion of $P(r)$ in (83), (100) and Now we have $\Phi_m^{(1)}(t) = \sqrt{2/\pi}t\sqrt{1-t^2}$ and so

$$X_r = \tfrac{1}{2}\pi\sqrt{2\pi}\omega\rho a^3(1+A_1)\sum_{m=0}^{\infty}\alpha_m^{(1)}\int_0^1 \Phi_m^{(1)}(t)\Phi_0^{(1)}(t)\frac{t}{(1-t^2)^{1/2}}\, dt = \omega\rho\tfrac{8}{15}\sqrt{2\pi}a^3(1+A_1)\alpha_0^{(1)} \tag{122}$$

after using (105) once again.

*4.3. Radiation problems*

We also briefly consider the generation of waves by the submerged plate moving in either heave or roll (about an axis coinciding with a diameter of the plate). The procedure we follow is similar to that used for scattering and broadly follow the modifications made for radiation in the two-dimensional case. Thus here we give simply the final expressions needed to compute the various quantities of interest.

We find that the added mass and radiation damping coefficients in vertical heave motion of unit amplitude, $\mathcal{A}^h$, $\mathcal{B}^h$ are given by

$$\frac{\mathcal{A}^h}{\pi\rho a^3} + \mathrm{i}\frac{\mathcal{B}^h}{\pi\omega\rho a^3} = \frac{8}{3\sqrt{\pi}}\left(\hat{A}_0^h\alpha_0^{(0)} + \alpha_0^h\right) \tag{123}$$

where $\hat{A}_0^h$ is given by

$$\hat{A}_0^h\left(1 - \mathrm{i}\pi\mu\sum_{m=0}^{\infty}\alpha_m^{(0)}F_m^{(0)}\right) = \mathrm{i}\pi\mu\alpha_0^{(0)}\frac{2}{3\sqrt{\pi}} \tag{124}$$

and $\alpha_0^h$ satisfies

$$\frac{\alpha_l^h}{(4l+3)} + \sum_{m=0}^{\infty}\alpha_m^h\widehat{K}_{ml}^{(0)} = \frac{2}{3\sqrt{\pi}}\delta_{l0}, \qquad l = 0, 1, \ldots \tag{125}$$

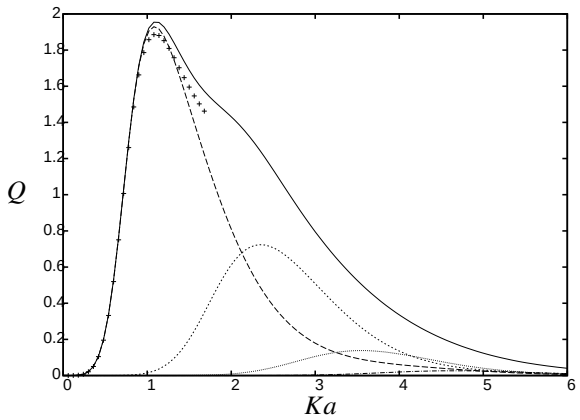


Figure 9. The variation of scaled scattering cross-section $Q$ (solid line) against $Ka$ for a submerged disc in infinite depth with $a/d = 2.5$. The plus symbols represent a one-term approximation to the solid line. Also shown are the first four modal components of $Q$ ordered left to right.

The far-field radiated waves are given by the function $A^h(\theta) = A_0^h$ where $A_0^h = a\mathrm{e}^{Kd}\hat{A}_0^h$.

In the case of roll, where the plate is given the vertical velocity distribution of $r\cos\theta$ the added inertia and radiation damping coefficients, $\mathcal{A}^r$, $\mathcal{B}^r$ are given by

$$\frac{\mathcal{A}^r}{\pi\rho a^5} + \mathrm{i}\frac{\mathcal{B}^r}{\pi\omega\rho a^5} = \frac{8}{15\sqrt{\pi}}\left(\hat{A}_1^r\alpha_0^{(1)} + \alpha_0^r\right) \tag{126}$$

where $\hat{A}_1^r$ is given by

$$\hat{A}_1^r\left(1 - \mathrm{i}\pi\mu\sum_{m=0}^{\infty}\alpha_m^{(1)}F_m^{(1)}\right) = \mathrm{i}\pi\mu\alpha_0^{(1)}\frac{4}{15\sqrt{\pi}} \tag{127}$$

and $\alpha_0^r$ satisfies

$$\frac{\alpha_l^r}{(4l+5)} + \sum_{m=0}^{\infty}\alpha_m^r\widehat{K}_{ml}^{(1)} = \frac{4}{15\sqrt{\pi}}\delta_{l0}, \qquad l = 0, 1, \ldots \tag{128}$$

The far-field radiated waves are given by the function $A^r(\theta) = 2\mathrm{i}A_1^r\cos\theta$ where $A_1^r = a^2\mathrm{e}^{Kd}\hat{A}_1^r$.

The two systems of equations (125), (128) are the same as (111) for $n = 0, 1$ but with different right-hand side terms.

### *4.4. Results*

In order to compare with the results of Farina & Martin [12] we need to rescale the scattering cross-section and have thus plotted $Q = 4\sigma/Ka$ against $Ka$. An infinite depth version of the formulation has also been used (the finite depth version presented above with a submergence of $d/h = 0.05$ gives almost identical results) and results are shown in figure 9–11 for $a/d = 2.5$, 10 and 100/6 corresponding to figures 3, 6 and 5 (respectively) in Farina & Martin [12].

There is good agreement with the results of Farina & Martin [12] for $Ka < 1.5$ but significant differences develop for larger values of $Ka$. Our results are fully resolved numerically and have converged to a high degree of accuracy. Thus we have required no more than a truncation to 6 terms in the series for $P_n(r)$ and 10 angular modes, and figures 9–11 illustrate this convergence by overlaying one, three and five term approximations to the fully converged results. We can only suggest that the differences are due to computational inaccuracies for higher frequencies in the results of Farina & Martin [12].

Spikes in the scattering cross-section are associated with resonances over the plate, as described by Miles [26] in a related problem, excited by the modal components of the incident wave and with frequencies $K = \omega^2/g = \kappa\tanh\kappa d$ characterised by the first radial zero of $J_m(\kappa a)$ for $m \geq 0$. For example, in figure 11 the first three spikes occur at $\kappa a \approx 2.18, 3.48, 4.66$ just below the zeros $2.40, 3.83, 5.13$ of the first zeros of $J_m(\kappa a)$. As $a/d$ increases the values of $\kappa a$ at which spikes appear get closer to the zeros of the Bessel functions and the spikes increasingly tall and narrow.

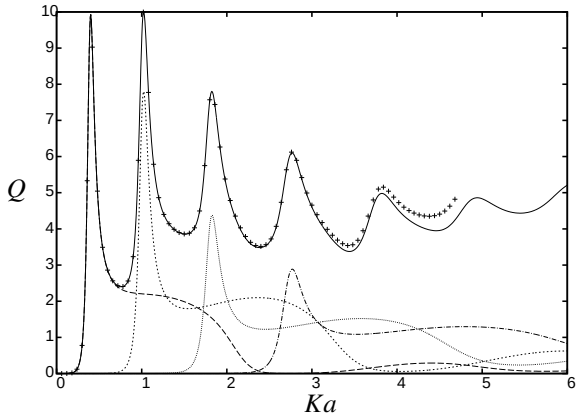


Figure 10. The variation of scattering cross-section $Q$ (solid line) against $Ka$ for a submerged disc infinite with $a/d = 10$. The plus symbols represent a three-term approximation. Also shown are the first four modal components of $Q$ ordered left to right.

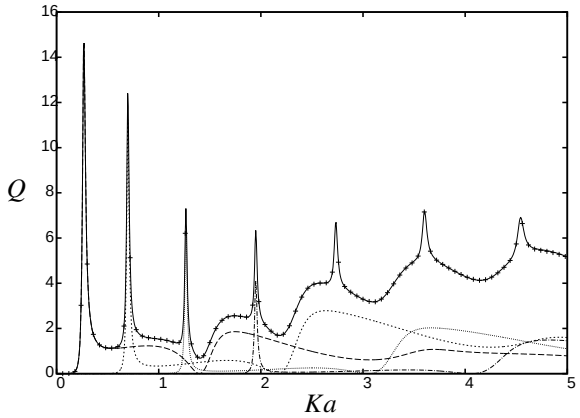


Figure 11. The variation of scattering cross-section $Q$ (solid line) against $Ka$ for a submerged disc in infinite depth with $a/d = 100/6$. The plus symbols represent a five-term approximation. Also shown are the first four modal components of $Q$ ordered left to right.

We have also shown in figure 12 and 13 the vertical heave force and roll moment (respectively) on a submerged disc in infinite depth for the same three sets of values of $a/d$ used in earlier scattering cross-section figures. Now the first $n = 0$ angular mode excites a large response in the heave force and the $n = 1$ angular mode similarly contributes to a large response in the roll moment both of which are amplified as the submergence depth is reduced, or $a/d$ is increased. We note superficial similarities with the force and moment computations of section 2 for two-dimensional plates which is not entirely unexpected, although it should be noted that in figures 3 and 4 each curve denoted a different finite depth ratio and a fixed frequency with respect to the depth was selected.

Finally, in figures 12, 13 we have illustrated some typical results for the dimensionless heave added mass and radiating damping coefficients $\mathcal{A}_h/(2\rho a^4)$ and $\mathcal{B}_h/(2\omega\rho a^4)$ against frequency and overlaid a plot of the heave diffracted wave force $\hat{X}_h$. As was noted previously in the two-dimensional problems of §2 and §3, the vanishing of the heave damping coefficient coincides with a zero of the heave wave force. Increasing the ratio of $a/d$ leads to an amplification in the added mass and radiation damping associated with the resonant motion of the fluid over the plate.

## 5. Conclusion

The scattering of incident waves and radiation of waves by forced motion by thin horizontal plates in two and three dimensions has been considered. The focus has been on the presentation of an efficient solution method based on

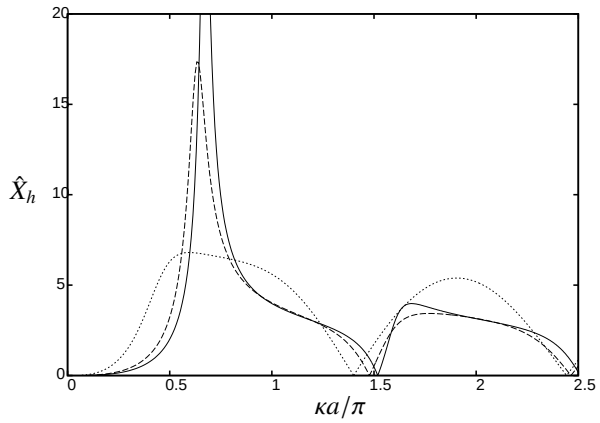


Figure 12. The variation of heave force $\hat{X}_h = |X_h|/(\rho\omega a^2)$ against $\kappa a/\pi$ on a submerged disc in infinite depth for $a/d = 100/6$ (solid line), $a/d = 10$ (dashed), $a/d = 2.5$ (dotted).

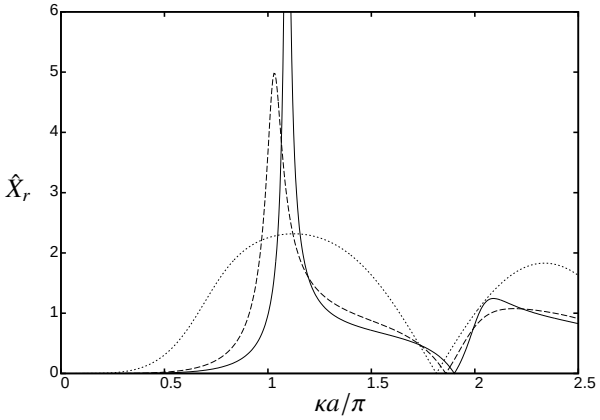


Figure 13. The variation of roll moment $\hat{X}_r = |X_r|/(\rho\omega a^3)$ against $\kappa a/\pi$ on a submerged disc in infinite depth for $a/d = 100/6$ (solid line), $a/d = 10$ (dashed), $a/d = 2.5$ (dotted).

Fourier/Hankel transforms. A Galerkin method applied to the solution of the integral equations which arise accurately captures the behaviour of the fluid at the edges of the plate. The final systems of equations and expressions for quantities of interest are very simple to compute accurately. It has been shown that only a few terms are needed in the truncated series expansion and a one-term truncation provides an effective low-frequency approximation.

An added benefit of the method is that we have not had to consider the roots of the dispersion relation either above or away from the plate. If the rigid impermeable plate were to be replaced by, for example, an elastic plate or a porous plate for which dispersion relations are complicated and roots hard to find, then the method outlined in the paper will apply.

Apart from algebraic complexity there is no fundamental difficulty in extending this transform approach to multiple horizontal plates. They would not have to lie in the same plane and they could overlap laterally. Certainly, in the latter case of overlapping plates, a traditional 'eigenfunction matching' approach would end up in some amount of difficulty.

Presently, the method is being extended in two directions. Firstly, by looking a finite and semi-infinite rectangular plates and, secondly, by placing the plates in the free surface.

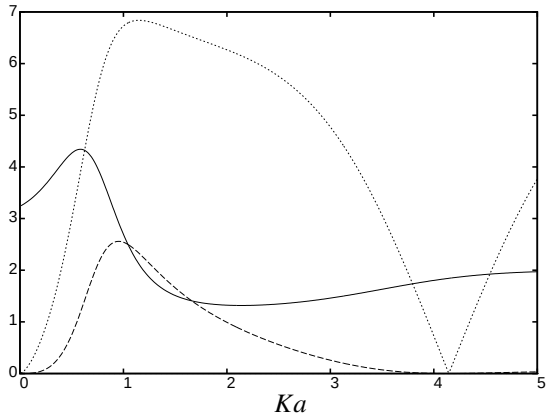


Figure 14. The variation of dimensionless heave added mass, $\mathcal{A}^h/(2\rho a^4)$ (solid line), radiation damping $\mathcal{B}^h/(2\rho\omega a^4)$ (dashed line) and heave force $|X_h|/(\rho\omega a^2)$ against $Ka$ for a submerged disc in infinite depth for $a/d = 2.5$.

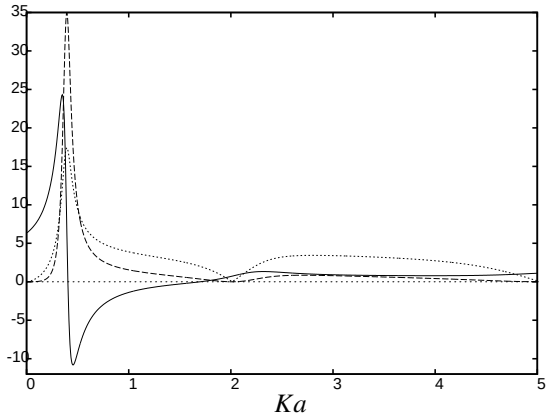


Figure 15. The variation of dimensionless heave added mass, $\mathcal{A}^h/(2\rho a^4)$ (solid line), radiation damping $\mathcal{B}^h/(2\rho\omega a^4)$ (dashed line) and heave force $|X_h|/(\rho\omega a^2)$ against $Ka$ for a submerged disc in infinite depth for $a/d = 10$.

## References

[1] McIver, M. Diffraction of water waves by a moored, horizontal, flat plate. J. Engng. Maths. 1985:8;279-301.
[2] Mahmood-Ul-Hassan, Meylan, M.H., Peter M.A. Water-wave scattering by submerged elastic plates, Q. J. Mech. Appl. Maths. 2009:62(3);321-344.
[3] Linton, C.M. & McIver, P. Handbook of Mathematical Techniques for Wave/Structure Interactions, Chapman & Hall CRC, 2001.
[4] Greene, T.H. & Heins, A.E. Water waves over a channel of infinite depth. Quart. Appl. Math. 1953:11;201-214.
[5] Heins, A.E. Water waves over a channel of finite depth with a submerged plane barrier. Quart. Appl. Math. 1950:11;201-214.
[6] Williams, T.D. & Meylan, M.H. The Wiener-Hopf and residue calculus solutions for a submerged semi-infinite elastic plate. J. Eng. Maths. 2012:75(1);81-106.
[7] Fernyhough, M. Applications of the residue and Modified Residue Calculus Method in linear acoustic and water wave theory. PhD thesis, University of Bristol, UK, 1994.
[8] Linton, C.M. The finite dock problem Z. angew. Math. Phys. 2001:52;640–656.
[9] Siew, P.F & Hurley, D.G. Long surface waves incident on a submerged horizontal plate J. Fluid Mech. 1977:83;141-151.
[10] Parsons, N.F. & Martin, P.A. Scattering of water waves by submerged plates using hypersingular integral equations. Appl. Ocean Res. 1992:14;313–321.
[11] Parsons, N.F. & Martin, P.A. Trapping of water waves by submerged plates using hypersingular integral equations. J. Fluid Mech. 1995:284;359-375.
[12] Farina & Martin, P.A. Scattering of water waves by a submerged horizontal disc using a hypersingular integral equation. Appl. Ocean Res. 1998:20(3);121-134.
[13] Porter, R. Scattering of surface waves by submerged cylinders of arbitrary cross-section. Proc. Roy. Soc Lond A. 2002:458;581-606.

[14] Grue, J & Palm, E. Reflection of surface waves by submerged cylinders Appl. Ocean Res. 1984;6(1):54–60.
[15] Song, A. & Faltinsen, O.M. Linear free-surface effects on a horizontally submerged and perforated 2D thin plate in finite and infinite water depths. Appl. Ocean Res. 2012;37: 220–234.
[16] Krenk, S. & Schmidt, H. Elastic Wave Scattering by a Circular Crack Phil. Trans. R. Soc. Lond. A. 1982:308(1502);167-198.
[17] Gradshteyn, I.M. & Ryzhik, I.S. Table of Integrals, Series and Products. Academic Press, New York, 2nd Edition, 1981.
[18] McIver, M., Evans, D.V. & Porter, R. Transparency of Structures in Water Waves. Proc 29th International Workshop on Water Waves & Floating Bodies, Osaka, Japan, 2014.
[19] Patarapanich, M. Forces and moments on a horizontal plate due to wave scattering. Coastal Engng. 1984:8;279-301.
[20] Mei, C.C. The Applied Dynamics of Ocean Surface Waves. World Scientific, Singapore, 1983.
[21] McIver, P. & Evans, D.V. The occurence of negative added mass in free surface problems involving submerged oscillating bodies J. Engng Maths. 1984:18;7-22.
[22] Martin, P.A. & Llewellyn-Smith, S.G. Generation of internal gravity waves by an oscillating horizontal disc. Proc. Roy. Soc. Lond. A. 2011:467;3406-3423.
[23] Tranter, C.J. A further note on dual integral equations and an application to the diffraction of electromagnetic waves. Q. J. Mech. Appl. Math. 1954:7;317-325.
[24] Krenk, S. A circular crack under asymmetric loads and some related integral equations. J. Appl. Mech. 1979:46;821-826.
[25] Maruo, H. The Drift of a Body Floating on Waves. J. Ship Res. 1960:4;1-10.
[26] Miles, J.W. Resonant amplification of gravity waves over a circular sill J. Fluid Mech. 1986:167;169-179.